Electronic Supplementary Material (ESI) for Journal of Materials Chemistry A.

Supplementary material to manuscript

Energy Landscapes in Alkali Aluminum Germanium Phosphate Glasses as probed by alkali proton substitution

Kevin Rein, Karl-Michael Weitzel

Chemistry Department, Philipps-Universität Marburg, 35032 Marburg, Germany

1. X-ray diffraction data of the AAGP glasses

To confirm the amorphicity of the three AAGP glasses, each glass batch has been analyzed via X-ray powder diffraction. The XRD spectra have been measured by a Philipps/Panalytical X'Pert Pro PW3040/60 device using the Co-K-α radiation. Figure S1, Figure S2 and Figure S3 show the XRD spectra of LAGP, NAGP and KAGP respectively. From the absence of sharp peaks it is concluded that the glass batches are amorphous.

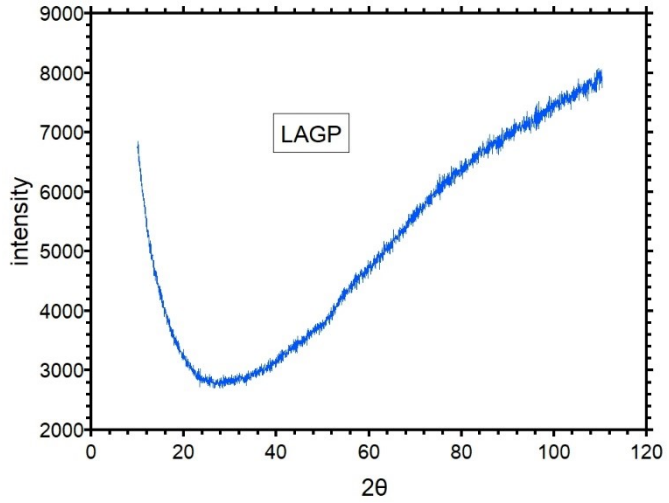

Figure S1: XRD spectrum of the LAGP glass.

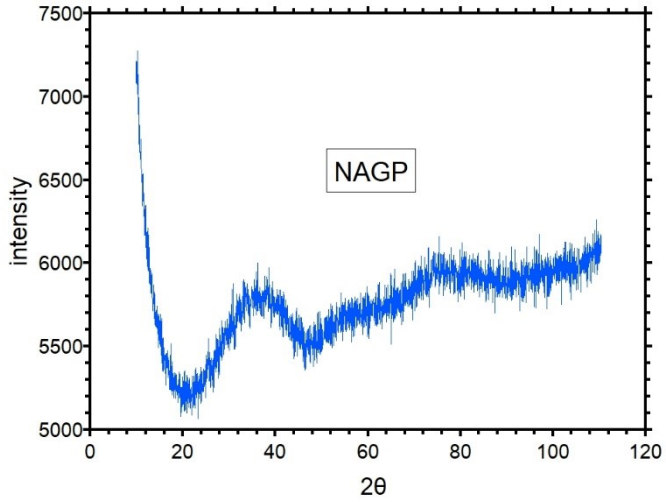

Figure S2: XRD spectrum of the NAGP glass.

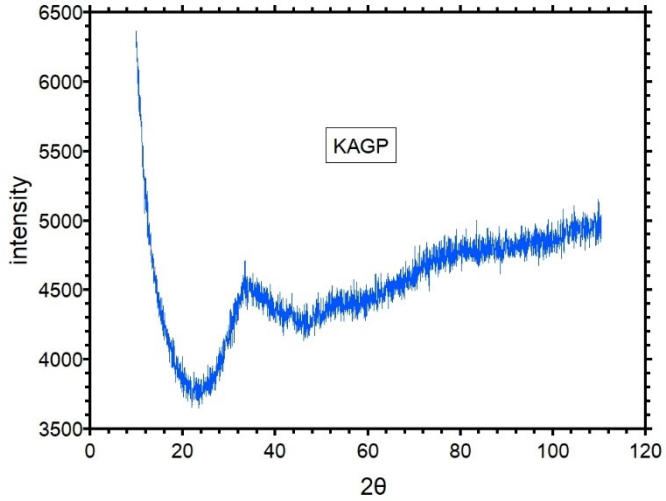

Figure S3: XRD spectrum of the KAGP glass.

2. Current time curves recorded during the APS experiments

One sample of each batch has been treated by an APS experiment. All experiments were carried out in a 200 mbar hydrogen atmosphere. Since the LAGP, NAGP and KAGP samples exhibit significantly different specific conductivities, running APS experiments at the same temperature and for the same time duration would lead to vastly different amount of charge transported. In order to ensure that the charge transport is large enough to allow analysis of the ToF-SIMS profiles the temperature and the experimental time have been increased in going from the LAGP to the NAGP and the KAGP, resulting in a total charge transported of 196 mC, 57 mC and 54 mC respectively. The current-time traces of all three samples investigated are shown in the following figures.

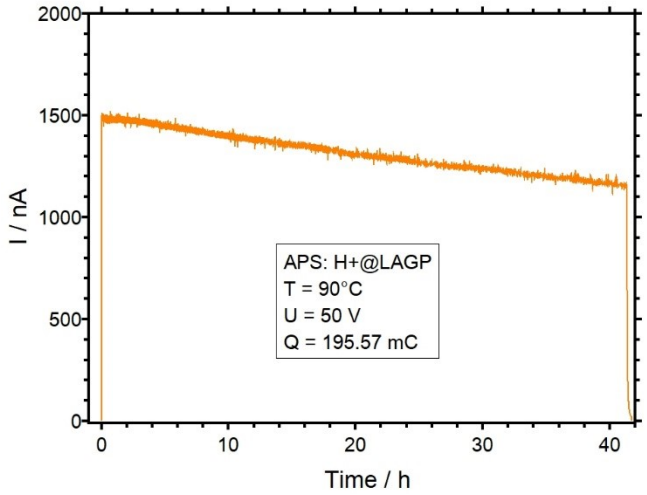

Figure S4: Current-time curve of the APS experiment on LAGP. The experimental conditions are given in the legend.

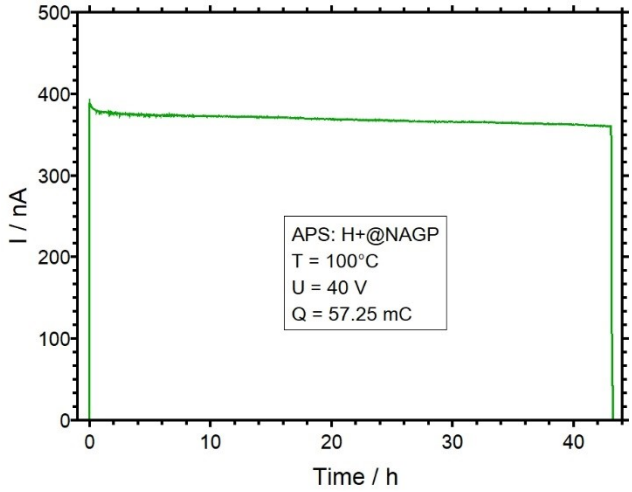

Figure S5: Current-time curve of the APS experiment on NAGP. The experimental conditions are given in the legend.

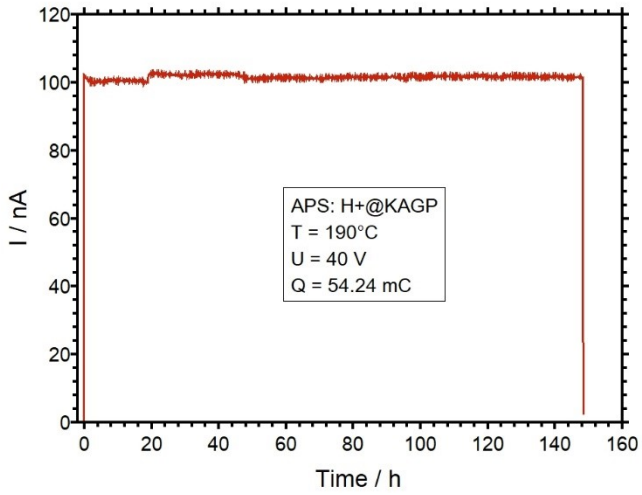

Figure S6: Current-time curve of the APS experiment on KAGP. The experimental conditions are given in the legend.

The three current-time curves show slightly different characteristics. The current drops over time in the case of LAGP and NAGP. For the KAGP, no change in the current over time can be seen. The small increase of current during t = 20 h and t = 40 h is most likely due to temperature fluctuations. The different behavior can be explained by a different ratio of the diffusion coefficients of the alkali ions and the hydrogen ions entering the material. When the diffusion coefficient of the ingoing hydrogen ions is far lower than the diffusion coefficient of the regarded alkali ion, a displacement zone will form beneath the anode, in which nearly all alkali ions are replaced by hydrogen ions. Since the current depends on the conductivity of the sample, a change in the conductivity in this displacement zone changes the total conductivity of the sample and therefore the current. The conductivity of the replacement zone is far lower than in the bulk of the material due to the low diffusion coefficient of hydrogen. With growing displacement zone, the total conductivity further decreases and therefore the current is decreasing. This is the case for LAGP and NAGP. When the diffusion coefficient of the hydrogen is not significantly lower than the diffusion coefficient of the alkali ion, some of the alkali ions remain in the displacement zone and will not be displaced. Moreover, the conductivity of the displacement zone does not change compared to the bulk conductivity and therefore the total conductivity of the material does not change significantly. As a result, the current does not change during the experiment. This is the case for KAGP and will be relevant for the theoretical analysis of the ion transport.

3. ToF-SIMS raw profiles

The raw data obtained by the ToF-SIMS analysis is represented by the intensity of a specific ion signal as a function of the sputter time. As described in the main text, the sputter time can be linearly translated to a depth. Figure S7, Figure S8, and Figure S9 show the raw data of the measured intensity of ionic species indicated as a function of the corresponding depth. These raw profiles are normalized by the procedure described in the next section.

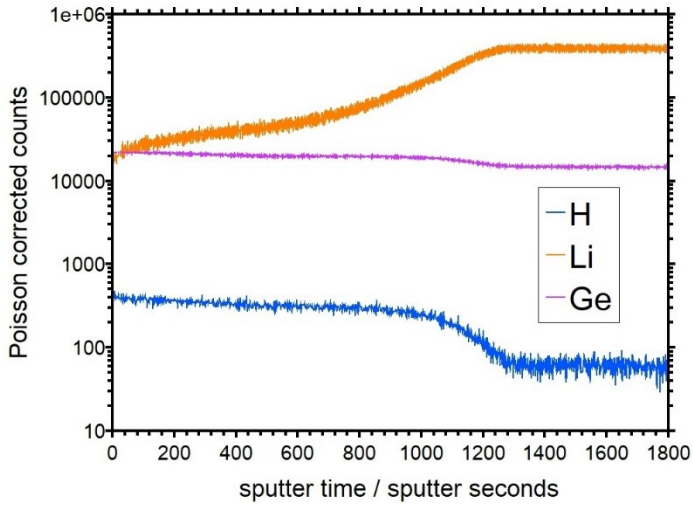

Figure S7: ToF-SIMS raw profile of the APS treated LAGP glass. The anode side is shown.

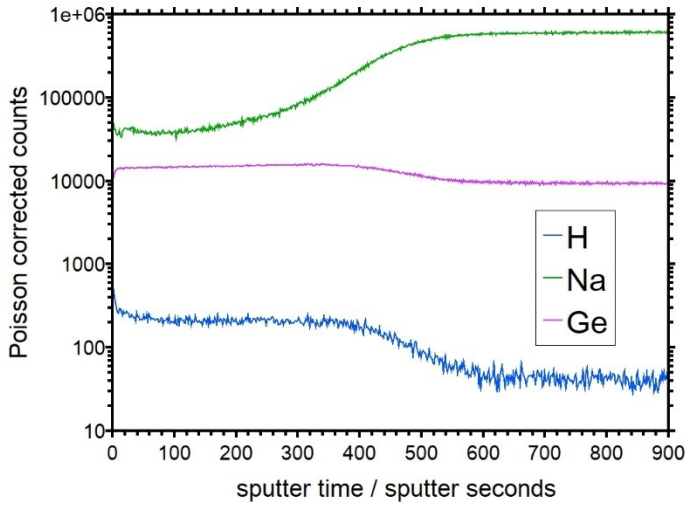

Figure S8: ToF-SIMS raw profile of the APS treated NAGP glass. The anode side is shown.

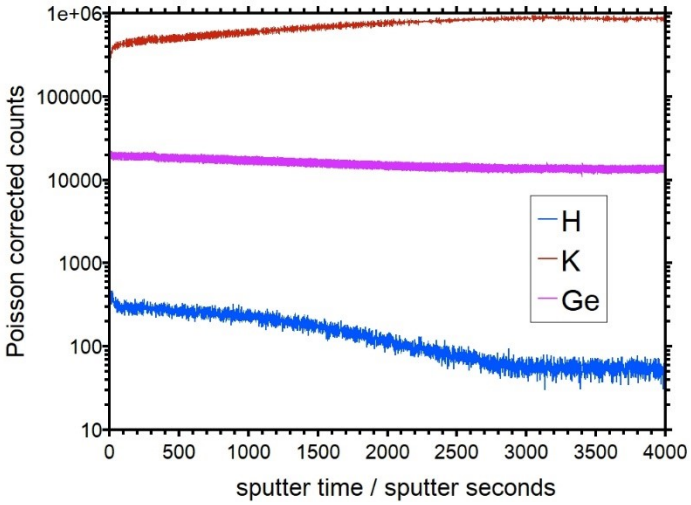

Figure S9: ToF-SIMS raw profile of the APS treated KAGP glass. The anode side is shown.

4. Normalization of the Concentration Depth Profiles

In order to analyze ion migration quantitatively, the profiles acquired by the ToF-SIMS analysis have to be normalized. The ToF-SIMS raw-data is in principle the intensity of a chosen ion signal as a function of the cycles sputtered. In a first step, the sputter cycles are translated to a depth. The depth is measured by a depth profilometer. Assuming a constant sputter rate, the depth is calibrated linearly. The next step is the normalization of the measured ion intensities to the corresponding ion concentration. Therefore, the ion concentration is set to be linearly dependent on the ion intensity. Contributions of the foreign ion to a change in the matrix of the glass are neglected. In the following we describe the normalization process of the concentration for an alkali glass with a mobile charge carrier A^+ and the foreign charge carrier H^+.

For the ion density $n_{A/H}(z)$ for the alkali ion A^+ respectively the hydrogen ion H^+ in the depth z the following applies:

	$n_A(z) = a \times I_A(z)$	(1)
	$n_H(z) = b \times I_H(z)$	(2)

Here, $I_{A/H}(z)$ is the measured intensity of the A^+/H^+ ion. The constant factors *a* and *b* scale the ion intensity. The factor *a* can easily be determined by the normalization of the bulk intensity of the alkali ion. In the bulk area, the density of A^+ ions is constant. Knowing the exact composition and the density of the glass, the ion density for the bulk can easily be calculated. Therefore, factor *a* can be calculated by dividing the A^+ bulk density of the glass by the averaged signal intensity in the bulk. The ion density of H^+ in the bulk is not zero. This can be due to remaining water from the synthesis or bound H^+ in form of O-H groups. The mean value of the H^+ intensity in the bulk is subtracted from the H^+ intensity $I_H(z)$ in all points z. This acts as a baseline correction. Since we assume charge neutrality each displaced alkali ion has to be replaced by a hydrogen ion. With setting the bulk ionic density arbitrarily to 1 we get as a boundary condition:

	$1 = a \times I_A(z) + b \times I_H(z)$	(3)

To achieve that the sum in equation (3) is near to 1 in all increments z, a least squares minimization is applied:

	$\frac{\partial}{\partial b}\sum_z \left(1 - a \times I_A(z) - b \times I_H(z)\right)^2 = 0$	(4)

The derivative results in the following for *b*:

	$b = \frac{\sum_z \left(I_H(z) - a \times I_A(z) \times I_H(z)\right)}{\sum_z I_H(z)^2}$	(5)

The normalized concentration depth profiles of the three glass samples are shown in Figure S10-S12.

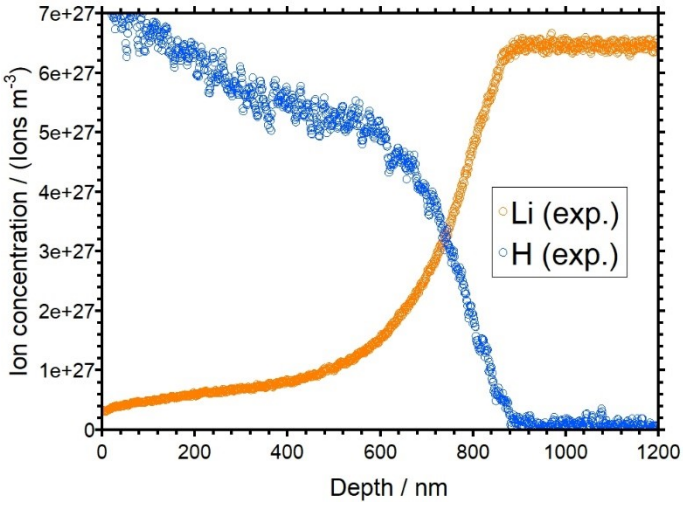

Figure S10: Normalized ToF-SIMS profile of the anode side of an APS treated LAGP sample.

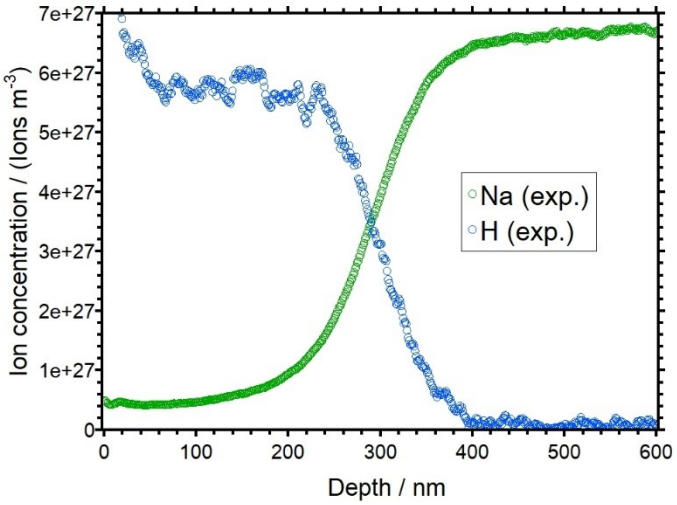

Figure S11: Normalized ToF-SIMS profile of the anode side of an APS treated NAGP sample.

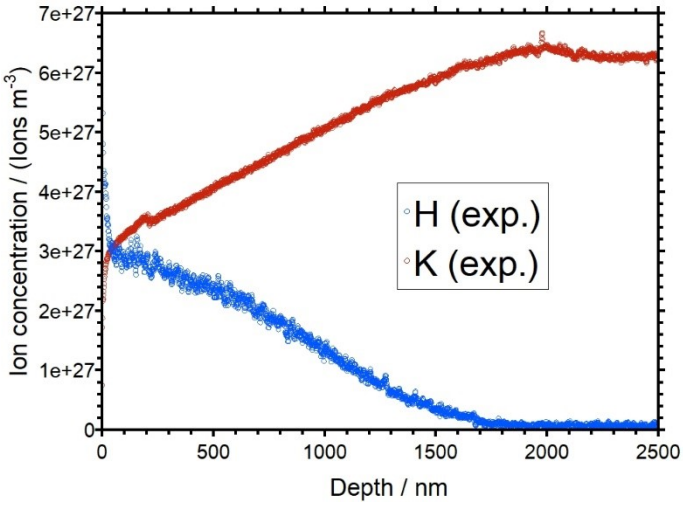

Figure S12: Normalized ToF-SIMS profile of the anode side of an APS treated KAGP sample.

5. Analysis of the precision of the simulation parameters for NAGP

The simulation parameters $D_{Na,0}$, D_H and Γ for the three AAGP glasses have been varied to analyze their influence on the simulated concentration depth profiles. As in the main text, the precision of the simulation parameter have been determined. The results are shown in Figure S13 to Figure S21.

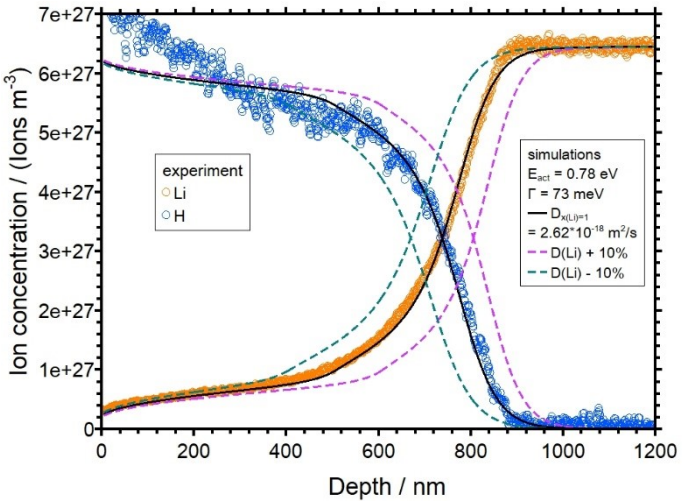

Figure S13: Simulated and experimental concentration depth profile for LAGP. The parameter $D_{Li,0}$ has been varied by ± 10%.

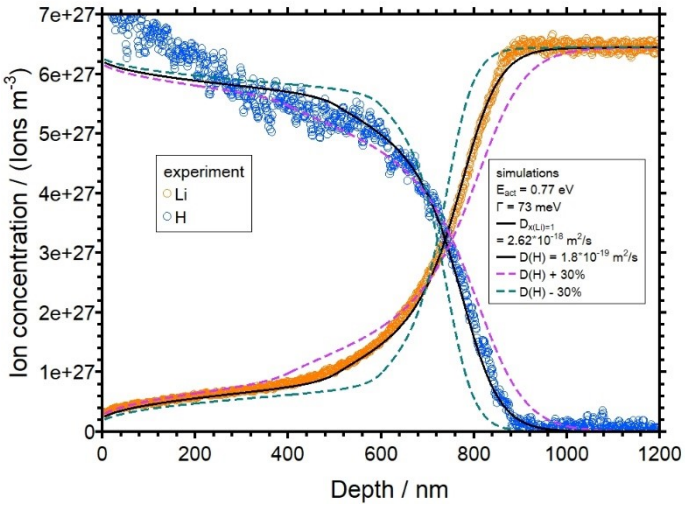

Figure S14: Simulated and experimental concentration depth profile for LAGP. The parameter D_H has been varied by ± 30%.

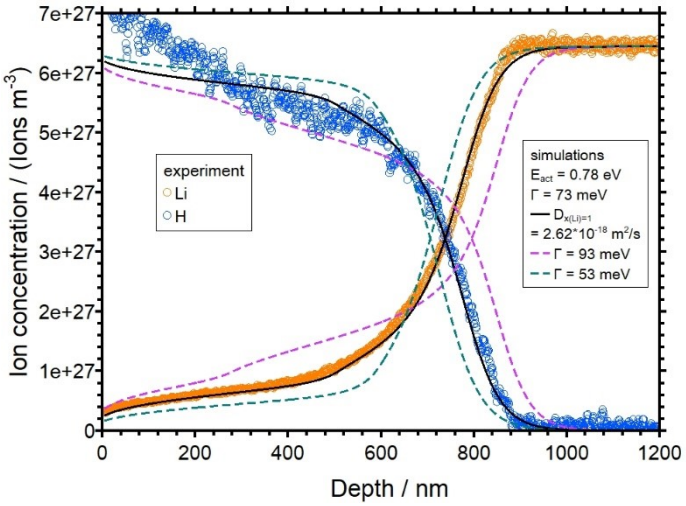

Figure S15: Simulated and experimental concentration depth profile for LAGP. The parameter Γ has been varied by ± 20 meV.

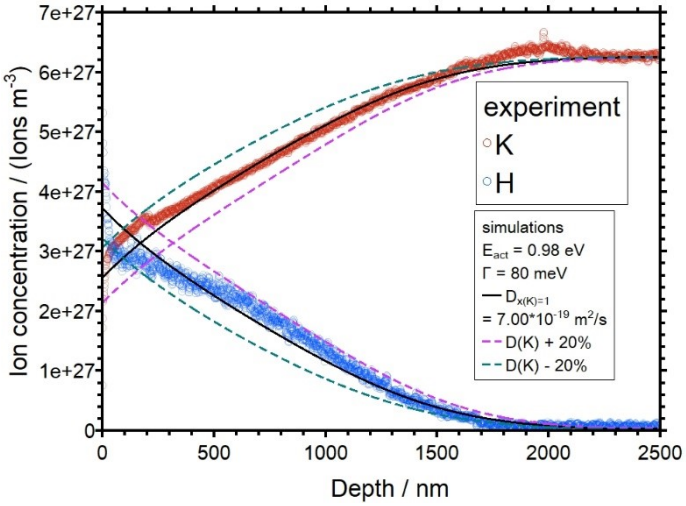

Figure S16: Simulated and experimental concentration depth profile for KAGP. The parameter $D_{K,0}$ has been varied by ± 20%.

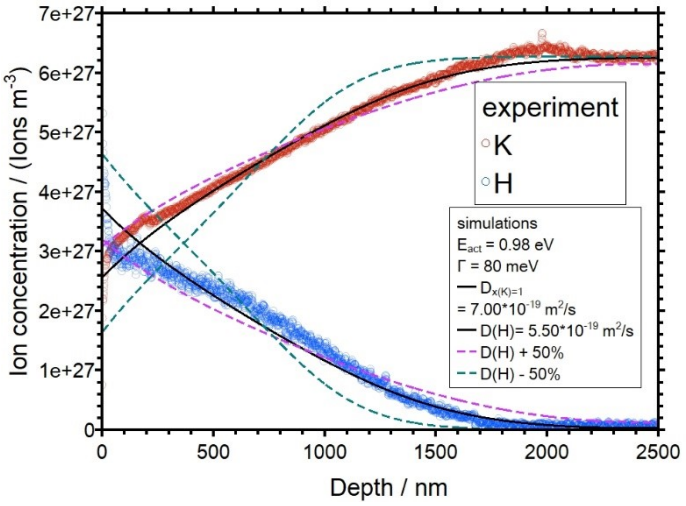

Figure S17: Simulated and experimental concentration depth profile for KAGP. The parameter D_H has been varied by ± 50%.

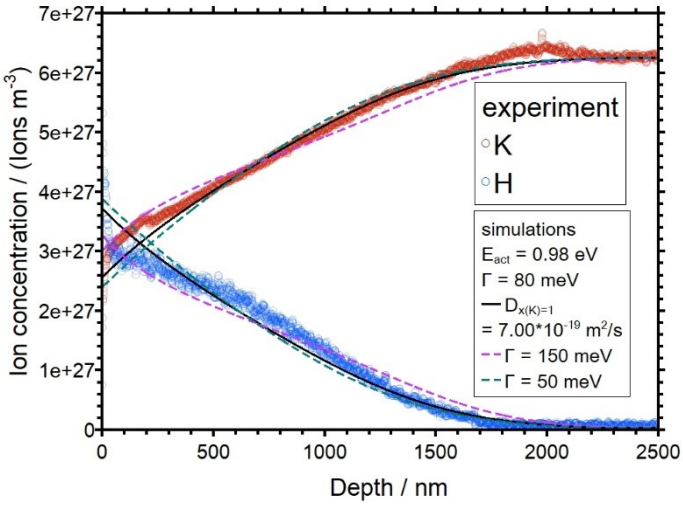

Figure 18: Simulated and experimental concentration depth profile for KAGP. The parameter Γ has been varied by ± 60 meV.

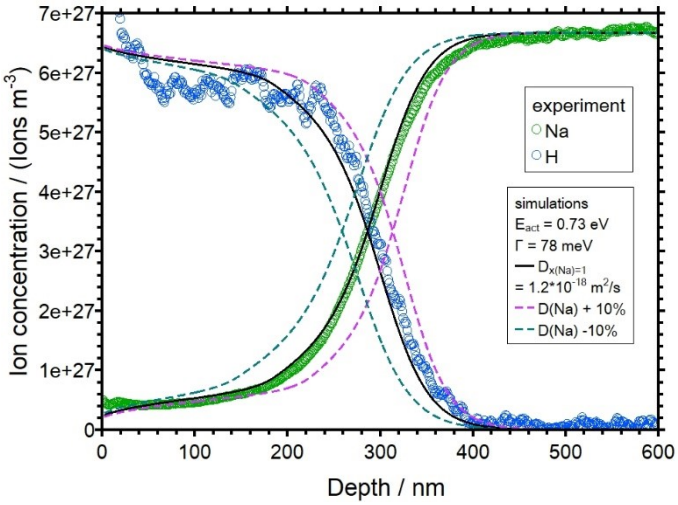

Figure S19: Simulated and experimental concentration depth profile for NAGP. The parameter $D_{Na,0}$ has been varied by ± 10%.

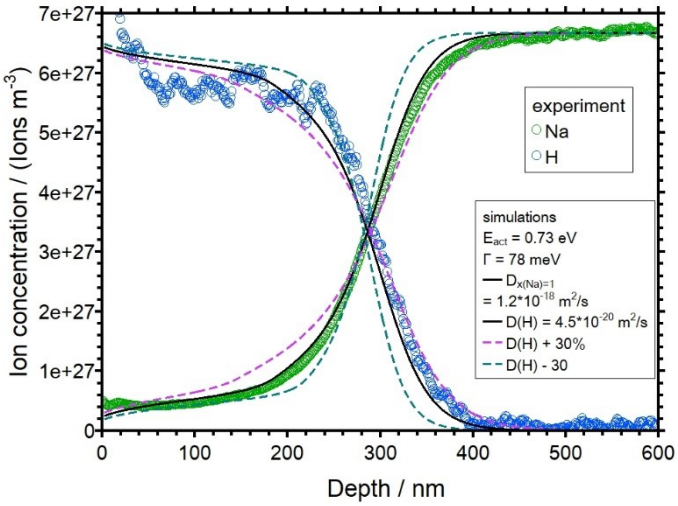

Figure S20: Simulated and experimental concentration depth profile for NAGP. The parameter $D_{H,0}$ has been varied by ± 30%.

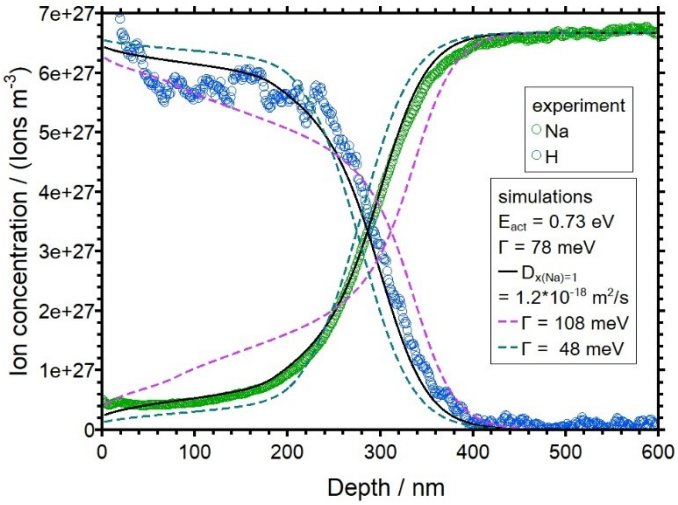

Figure S21: Simulated and experimental concentration depth profile for NAGP. The parameter Γ has been varied by ± 30 meV.